Available online at www.sciencedirect.com
SCIENCE DIRECT®
Polymer 45 (2004) 2211–2219
polymer
www.elsevier.com/locate/polymer

Submicrometer-scale heterogeneous surfaces by PS–PMMA demixing

C.M. Dekeyser[a,b], S. Biltresse[b], J. Marchand-Brynaert[b], P.G. Rouxhet[a], Ch.C. Dupont-Gillain[a,*]

[a]*Unité de Chimie des Interfaces, Université catholique de Louvain, Croix du Sud 2/18, 1348 Louvain-la-Neuve, Belgium*
[b]*Unité de Chimie Organique et Médicinale, Université catholique de Louvain, Place Louis Pasteur 1, 1348 Louvain-la-Neuve, Belgium*

Received 14 August 2003; received in revised form 13 January 2004; accepted 16 January 2004

Abstract

Patterned surfaces were created using two polymers: polystyrene (PS) on the one hand, and either poly(methyl methacrylate) (PMMA) or poly(methyl methacrylate)–poly(methacrylic acid) (PMMA–PMAA) on the other hand. PMMA was dissolved in a solvent of PS; this solution was then spin-coated on a PS support that partially dissolved during the process. The materials were analyzed by water contact angle measurement, XPS, ToF-SIMS and AFM. The effect of the solvent on the final surface morphology was strongly marked. With chloroform, the acrylic polymer was the major surface constituent, possibly because of the high evaporation rate of this solvent. With toluene, which is a better solvent for PS compared to PMMA, the obtained surface was almost exclusively constituted of PS. The use of chlorobenzene provided inclusions of acrylic polymer in PS, both polymers being exposed at the outermost surface. The surface morphology presented rings, the interior of which consisted of the acrylic polymer, while the rest of the surface was made of PS.

Keywords: Surface heterogeneity; PS–PMMA; Spin-coating

1. Introduction

Most polymers are immiscible, due to chain length and segment connectivity which are at the origin of a very low mixing entropy. Many studies [1,2] were performed concerning the phase separation in bulk polymer materials. However, the nature of the surface is also important for many applications, such as coatings and biocompatible materials. In the field of surface biocompatibility, it has been shown that cells respond to chemically and topographically heterogeneous surfaces [3].

Polystyrene–poly(methyl methacrylate) (PS–PMMA) is a well-known immiscible blend that has been extensively studied after spin-coating on a substratum, using a variety of conditions. Ton-That et al. [4] studied the influence of the concentration and composition of PS–PMMA blends on the morphology and composition of the surface of films spin-coated from solutions in chloroform. In all cases, the surface was enriched with PMMA, due to its higher solubility in chloroform compared to PS. Pits were observed with PMMA mole fractions less than 50%, the size of the pits increasing both with film thickness and PMMA concentration. For PMMA mole fractions above 50%, granular morphologies were obtained. Upon annealing above the glass transition temperatures of the two polymers, the influence of the solvent was removed or at least reduced. Surface enrichment of the PS component then occured due to minimizing of the polymer–air interfacial free energy [5].

The chemical nature of the substratum also greatly influences the surface morphology. Different film thicknesses were obtained by varying the polymer concentrations in toluene [6]. In the case of thick films (25 μm), a PS-rich overlayer was formed and the surface structure did not depend on the substratum characteristics. For ultrathin films (10 nm), no distinct phase-separated surface structure and also no dependence on the substratum characteristics were observed because of the small thickness of such films (less than twice the gyration radius of an unperturbed chain). For films of 100 nm thickness, a well-defined sea-island-like phase-separated structure was observed at the film surface where both PS and PMMA-rich phases were observed. The PMMA domain size and shape were dependent on the substratum, the PMMA concentration at the air–polymer interface decreasing with an increase in substratum hydrophilicity. The same observation was made for PS–PMMA

* Corresponding author. Tel.: +32-10-473592; fax: +32-10-472005.
E-mail address: dupont@cifa.ucl.ac.be (C.C. Dupont-Gillain).

0032-3861/$ - see front matter © 2004 Elsevier Ltd. All rights reserved.
doi:10.1016/j.polymer.2004.01.045

blends spin-coated from solutions in tetrahydrofuran (THF) [7].

Walheim et al. [7] used different solvents (toluene, THF and methyl ethyl ketone (MEK)) for the spin-coating process in order to compare their effect on the surface morphology. In an intermediate evaporation stage, the more soluble phase was swollen with the solvent, which gave, after final evaporation, protruding domains of the less soluble polymer. If the solvent is better for the polymer which has the lower surface energy, the surface structure exhibits sharp edges. In the opposite case, rather round surface structures are obtained.

The influence of chain-ends is also not to be neglected. If the surface free energy is lower for the end groups than for the main chain part, the former are preferentially located at the surface [8]; this explains a possible influence of the molecular mass. However, the latter may also affect the film properties through another mechanism, i.e. the fact that a polymer chain at the surface has a smaller conformational entropy. As a longer polymer chain at the surface suffers a more severe conformational entropy penalty, the surface is more favorably covered by the component with a lower molecular mass. For PMMA with a very low molecular mass compared to PS, PMMA was preferentially segregated at the film surface, even though it has a higher surface energy than PS [9]. Moreover the PMMA surface fraction decreased with an increase of PMMA molecular mass.

In this study, we used the spin-coating of a polymer on top of another polymer substratum that dissolves during the process. As a result, a blend of the two polymers is obtained at the surface of the support. Different concentrations and solvents were considered. A copolymer of poly(methyl methacrylate)–poly(methacrylic acid) (PMMA–PMAA) was also used instead of PMMA in order to bring reactive sites at the interface, with the aim to chemically modify the polar surface zones in a subsequent work. The two main techniques used for surface characterization were atomic force microscopy (AFM) and X-ray photoelectron spectroscopy (XPS). AFM allows a surface to be imaged on the nanometer scale, based on topography or friction contrasts (LFM, lateral force microscopy). XPS gives the chemical composition of a surface layer of a few nanometers. Water contact angles were also measured. Finally, time-of-flight secondary ion mass spectroscopy (ToF-SIMS) analyses were performed to characterize the composition of the outermost surface (about one molecular layer).

2. Materials and methods

2.1. Sample preparation

The PMMA used, provided by Aldrich (USA), had a M_w of 996,000 and a glass transition temperature (T_g) of 125 °C (given by the supplier). The random copolymer of PMMA–PMAA, provided by Aldrich, USA, had a molar ratio MMA/MAA of 62, $M_w = 34,000$, and $M_n = 15,000$ (given by the supplier).

Different PMMA or PMMA–PMAA solutions were prepared by dissolving the polymer in various solvents at three concentrations: 0.1, 1 and 10 g/l. Three solvents were used: chloroform (Merck, Germany), toluene and chlorobenzene (both from Scharlau Chemie, Spain). PS disks of 12 mm diameter were cut off from Petri dishes (Greiner Labortechnik, Germany). The PS used has a M_w of ~220,000 and a M_n of ~120,000 (characterized by gel permeation chromatography, GPC). The disks were cleaned by ultrasound treatment in isopropanol for 1 min and dried under nitrogen flow. Spin-coating of the PMMA or PMMA–PMAA solutions on top of the PS substrata was performed as follows: the rotation of the PS disk was switched on (under N_2 flow, acceleration = 20,000 rpm/s, speed = 5000 rpm), then 30 μl of the PMMA solution were immediately deposited on the PS, with an angle of 45° between the pipette and the sample; the rotation was stopped after 60 s.

Pure PMMA and PMMA–PMAA were analyzed after spin-coating on microscope cover glasses (diameter = 15 mm; Menzel-Gläser, Germany); the solvent used was toluene for PMMA and chlorobenzene for PMMA–PMAA. PS was characterized after spin-coating of pure chlorobenzene to smooth the surface (same spin-coating parameters as before).

In order to localize the PMMA–PMAA domains at the sample surface, selective dissolution of the copolymer versus PS was achieved. The samples were immersed in 15 ml acetic acid (96% p.a., Merck, Germany) for 2 h. They were then rinsed and washed during 1 h in Milli-Q water (Millipore, Molsheim, France). After drying with N_2 flow, the samples were analyzed by AFM.

2.2. Surface characterization

The samples were imaged by AFM (Nanoscope III, Digital Instruments, Santa Barbara, USA) in contact mode under Milli-Q water at room temperature. The tip used was made of Si_3N_4, had a typical spring constant of 0.01 N/m and a typical radius of curvature of 20 nm (Park Scientific Instruments, Mountain View, USA). The scan rate was about 5 Hz and the applied force was the minimal value allowing to keep the contact between tip and sample. For each scanned area, images in height mode (trace and retrace) and images in lateral force mode (trace and retrace) were recorded.

Static water contact angles were measured by the sessile drop method. The instrument, using a CCD camera and an image analysis processor, was purchased from Electronisch Ontwerpbureau De Boer (The Netherlands). The drop size was 0.3 μl; the contact angle value was read after 5 s. For each sample, the determination was performed by averaging the results obtained on at least 10 droplets.

XPS spectra were recorded using an X-probe spec-

trometer (model SSX-100/206 from Surface Science Instruments) equipped with an aluminum anode (10 kV, 12 mA) and a quartz monochromator. Charge stabilization was achieved using an electron flood gun set at 8 eV and placing a grounded nickel grid 3 mm above the sample surface. The analyzed area was about 1.4 mm^2. The angle between the normal to the sample surface and the direction of the photoelectron collection was 55°. The order of peak analysis was: survey scan, C_{1s}, O_{1s} and C_{1s} again. No alteration of the C_{1s} peak shape under X-ray irradiation was noticed. The binding energy scale was set by fixing the component due to carbon only bound to carbon and hydrogen at 284.8 eV. A linear background subtraction was used. Intensity ratios were converted into molar concentration ratios by using the sensitivity factors proposed by the manufacturer (mean free path varying according to the 0.7^{th} power of photoelectron kinetic energy; Scofield cross-sections; constant transmission function).

Positive and negative ToF-SIMS spectra were obtained using a TFS 4000 MMI time-of-flight secondary ion mass spectrometer (Charles Evans, Redwood, California, USA). A pulsed gallium ion beam (940 pA, pulse rate 11 kHz, pulse time 1.5 ns) was swept over a 120×120 μm^2 area (positive spectra) or 180×180 μm^2 (negative spectra). The secondary ions were extracted at 3 keV acceleration voltage, with a post-acceleration of 7 keV. A grounded stainless steel grid covered the sample. During the acquisition time of 5 min, the total ion dose of 3.1×10^{12} Ga^+/cm^2 (positive spectra) or 3.1×10^{11} Ga^+/cm^2 (negative spectra) insured static conditions.

3. Results

The results obtained for the three pure polymers (PS disks and PMMA, PMMA–PMAA spin-coated on glass) are presented in Table 1 (first part). The water contact angles of PMMA and PS are close to those reported in the literature [10,11]. The O/C ratio measured by XPS reveals traces of contaminants for PS, is very close to the expected value for PMMA, and is a little lower than the expected value for PMMA–PMAA. ToF-SIMS spectra of PS (Fig. 4(a)) and PMMA (not shown) were similar to those reported in the literature [12].

The effect of the concentration of PMMA in the three solvents was investigated for PMMA spin-coated on PS. Three concentrations of PMMA in the different solvents were tested: 0.1, 1 and 10 g/l. At the two lower concentrations, no difference in terms of surface chemical composition and contact angle was noticeable with respect to pure PS, except for one sample, prepared from a concentration of 1 g/l in chloroform. In the same way, the AFM images showed no relief, and no friction contrast. When rising the concentration to 10 g/l, the water contact angle and XPS data were significantly different from those of pure polymers and varied according to the solvent used, as shown by Table 1. This last concentration was therefore used in order to investigate the effects of the solvents on the surface formed.

The surface obtained using chloroform presented a marked granular relief which was reflected in the friction image (Fig. 1); the water contact angle was lower than that of PMMA and the C and O mole fractions showed that PMMA was the major surface constituent. The AFM images obtained with toluene showed rings which corresponded to inclusions in the friction images (Fig. 1); the water contact angle and the C and O concentrations were close to those obtained for PS. Finally, the images obtained with chlorobenzene also showed rings which corresponded to a light friction contrast (Fig. 1); note that images obtained on the same sample showed a variation in the size and number of inclusions. The water contact angle was intermediate between those of PS and PMMA. The O/C ratio was 0.06, to be compared with 0.007 for PS and 0.42 for PMMA.

A set of experiments was performed by spin-coating PMMA–PMAA on PS from solutions at three concentrations (0.1, 1 and 10 g/l) in toluene. The results (chemistry, topography, contact angle) obtained for the two lower concentrations were again not very different from the data typical of PS. The copolymer was then spin-coated at the concentration of 10 g/l in the three different solvents. The results obtained are presented in Table 1 and Fig. 2. The

Table 1
Water contact angle and XPS data for pure polymers (PS disks and PMMA, PMMA–PMAA spin-coated on glass), and for PMMA or PMMA–PMAA spin-coated on PS from solutions (10 g/l) in various solvents

	Pure polymers			PMMA on PS			PMMA–PMAA on PS		
	PS	PMMA	PMMA–PMAA	Chloroform	Toluene	Chlorobenzene	Chloroform	Toluene	Chlorobenzene
θ_w [a]	90.7° (0.7°)	77.3° (0.7°)	70.4° (1.1°)	70.4° (1.4°)	88.4° (1.0°)	82.0° (4.1°)	64.1° (0.8°)	90.3° (0.7°)	85.0° (0.5°)
% C [b]	99.3	70.5	76.0	76.9	98.3	94.2	77.7	97.5	93.2
% O [c]	0.7	29.5	24.0	23.0	1.7	5.8	22.3	2.6	6.8
O/C × 100	0.7	42	31	30	1.8	6.2	29	2.6	7.3

[a] Standard deviation is given between brackets (10 measurements at least).
[b] Mole fraction C/(C + O).
[c] Mole fraction O/(C + O).

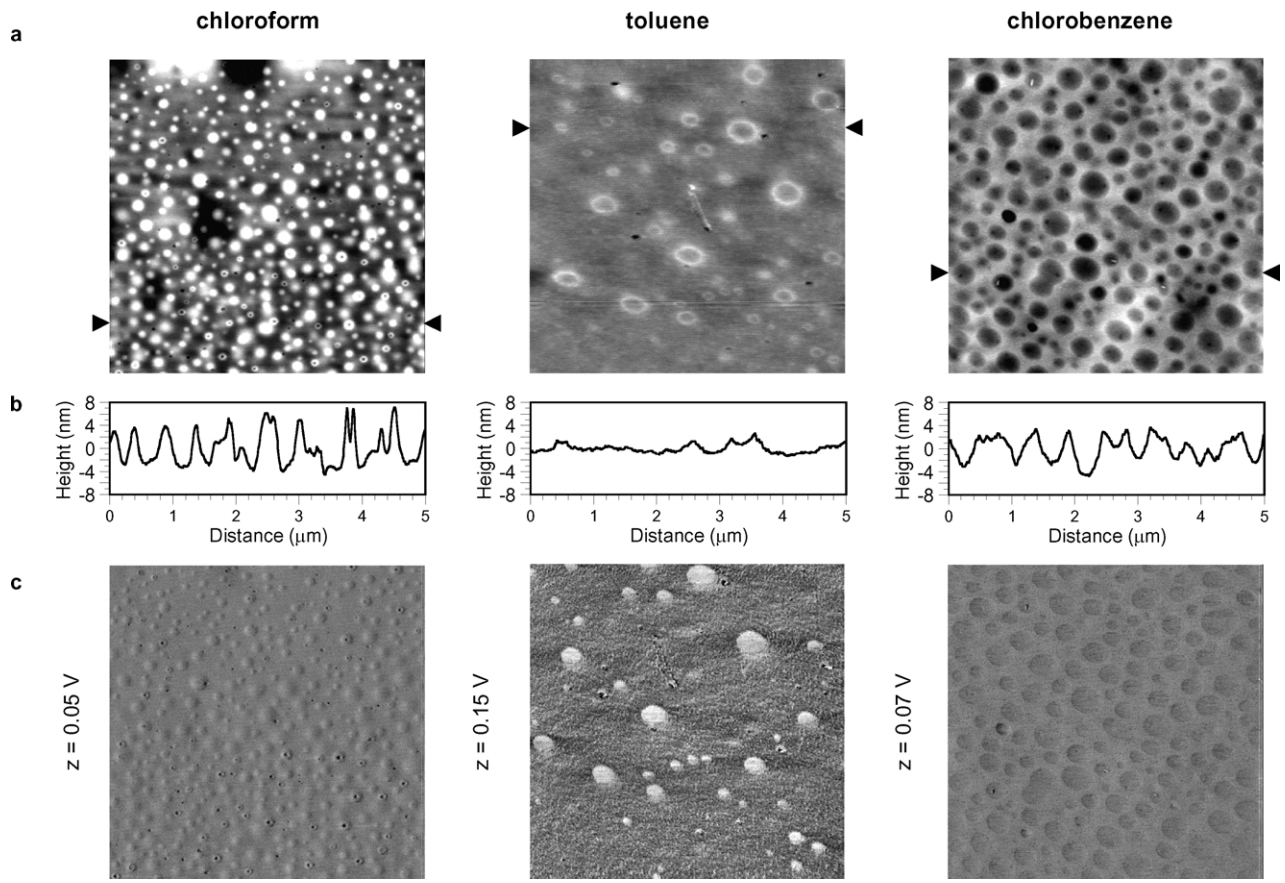

Fig. 1. AFM images ($5 \times 5\ \mu m^2$) obtained after spin-coating PMMA on PS from solutions (10 g/l) in different solvents. (a) Height (z-range = 10 nm); (b) section (indicated by the arrows in the height images); (c) friction (retrace, z-range indicated near the image).

AFM images of PMMA–PMAA spin-coated from chloroform solutions showed a film with holes (Fig. 2); the water contact angle was lower, even lower than that of PMMA–PMAA alone; the C and O mole fractions showed that the copolymer was the major constituent at the surface. With toluene, the water contact angle and the C and O concentrations were close to the values obtained for PS; the AFM images were similar to those obtained by spin-coating PMMA on PS. Finally, the samples prepared with chlorobenzene showed intermediate water contact angle and C and O concentrations; the AFM images were also similar to those obtained by spin-coating PMMA on PS but the friction contrast was stronger.

The C_{1s} peaks obtained after spin-coating PMMA–PMAA on PS from solutions at 10 g/l in the three solvents are presented in Fig. 3(b). Fig. 3(a) gives the C_{1s} peaks of pure PS and pure PMMA–PMAA, for the sake of comparison. For the samples prepared using chloroform, the carbon peak was similar to that of pure PMMA–PMAA. When toluene was used, the peak was similar to that of PS. Finally, for the samples made using chlorobenzene, the spectrum clearly showed a contribution of both polymers, PS and PMMA–PMAA, with the ester component near 289.0 eV and the shake up of PS near 291.5 eV.

From these results, it appears that the surfaces made using chloroform are principally covered with the acrylic polymer, the surfaces made using toluene consists principally of PS, whereas both PS and the acrylic polymer are clearly found at the surfaces obtained using chlorobenzene.

Assuming that the PMMA proportion does not vary as a function of depth, the PMMA surface fraction can be computed from the measured C and O concentrations. If the surface is considered as made of patches of PS and PMMA, and if the differences of density and (C + O) concentrations between the pure polymers are neglected, the O/C ratio of the sample can be expressed as:

$$\left(\frac{O}{C}\right)_{exp} \approx \frac{xO_{PA} + (1-x)O_{PS}}{xC_{PA} + (1-x)C_{PS}},$$

where x is the PMMA surface fraction. O_{PS} and O_{PA} are the oxygen concentrations, and C_{PS} and C_{PA} are the carbon concentrations in pure PS and pure PMMA, respectively, as deduced from XPS spectra of the pure polymers (Table 1). The PMMA surface concentration calculated by this equation for the surface obtained by spin-coating a 10 g/l solution in chloroform, toluene and chlorobenzene is equal to 77.7, 3.7 and 17.8%, respectively.

Fig. 4(c) presents the ToF-SIMS spectrum of a sample prepared by spin-coating a PMMA–PMAA solution in chlorobenzene and allows a comparison to be made with PS

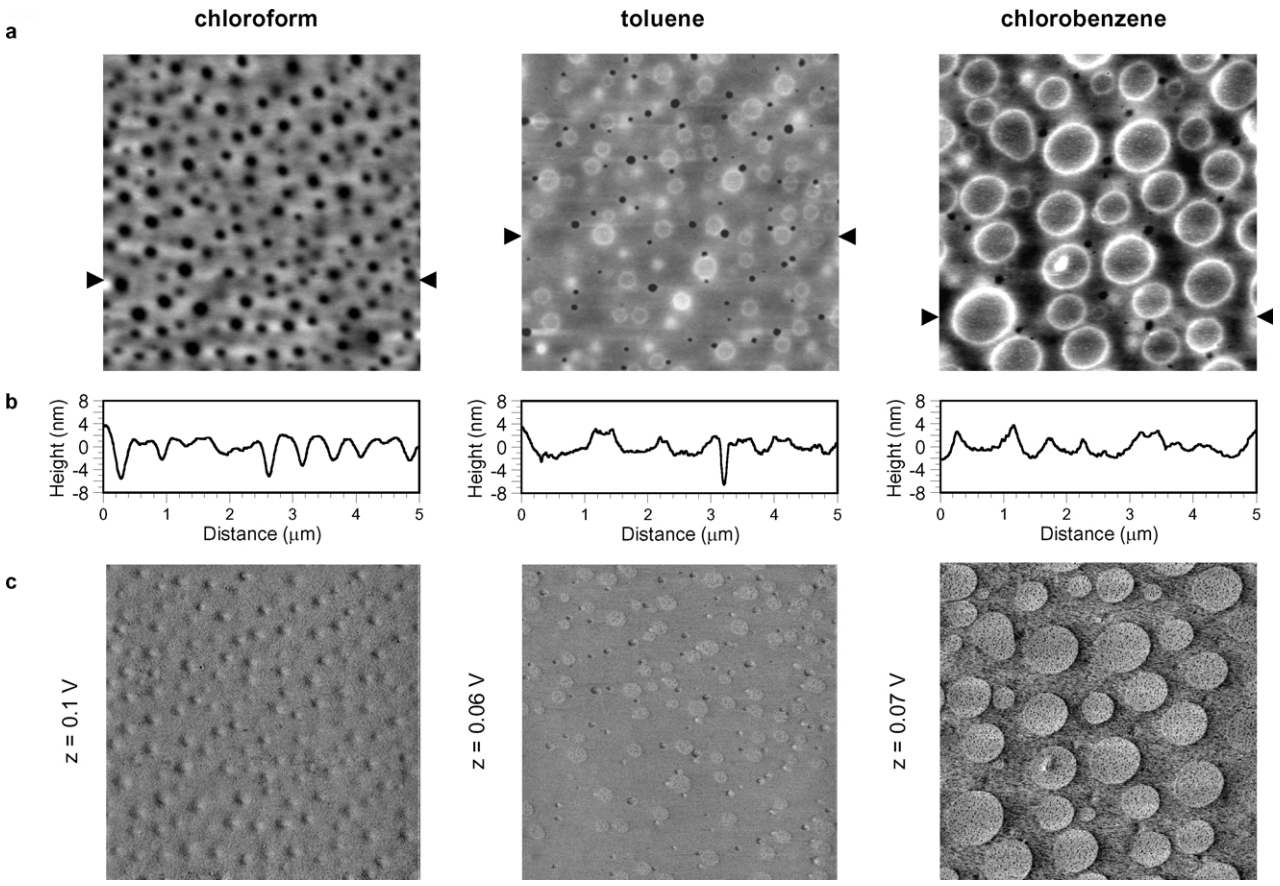

Fig. 2. AFM images ($5 \times 5\ \mu m^2$) obtained after spin-coating PMMA–PMAA on PS from solutions (10 g/l) in different solvents. (a) Height (z-range = 10 nm); (b) section (indicated by the arrows in the height images); (c) friction (retrace, z-range indicated near the image).

(Fig. 4(a)) and PMMA–PMAA (Fig. 4(b)). The peaks which are characteristic of each polymer are labeled in the reference spectra, such as tropylium ion (91) and related fragments (77, 51) due to the aromatic cycle of PS, and fragments related to the ester function of PMMA (69, 59, 45, 31). These peaks are all found in the spectrum of the sample obtained by spin-coating of PMMA–PMAA on PS from a solution in chlorobenzene, which confirms that both polymers are present at the outermost surface of this sample.

The repeatability of the patterns obtained was examined by preparing six samples under similar conditions, i.e. spin-coating of PMMA–PMAA (10 g/l in chlorobenzene) on PS plates, and by analyzing up to 16 areas of each sample by AFM. The surface structures were always present, but their size and concentration varied, the diameter of the rings being comprised between 150 nm and 1.5 μm. Examples of two extreme situations are presented in Fig. 5. In the AFM friction images, the contrasts are inverted between trace and retrace, indicating that the contrast is due to true friction and not to relief [13,14]. There was no significant correlation between the morphology and the position on the sample. The surface fraction represented by the inclusions was calculated using an image analysis software (Visilog, version 5.2 advanced Noesis, Courtaboeuf, France) and found to be in the range of 10 to 30%; this is in fair agreement with the PMMA–PMAA surface coverage calculated from XPS spectra. Thus, the inclusions are essentially made of PMMA–PMAA.

After selective dissolution of the PMMA–PMAA domains in acetic acid, the sample surface was imaged again by AFM (Fig. 6). The images showed holes, with a depth varying from 100 to 500 nm, confirming that the inclusions were made of PMMA–PMAA. The edges of the rings were still visible on the images, indicating that these edges were made of polystyrene and that the copolymer was located inside the rings observed in the AFM height images (Figs. 2 and 5).

4. Discussion

The solvents considered in this study are all good solvents of PS. Therefore, when a drop of solvent containing PMMA or PMMA–PMAA is deposited on the PS disk, a partial dissolution of PS occurs. At the same time, the solvent spread on the disk evaporates at a high rate because of the spinning and of the large surface exposed to air. This evaporation produces an increase of the concentration of the solution and a rise of its viscosity. Because the two polymers are not miscible, a phase separation occurs at

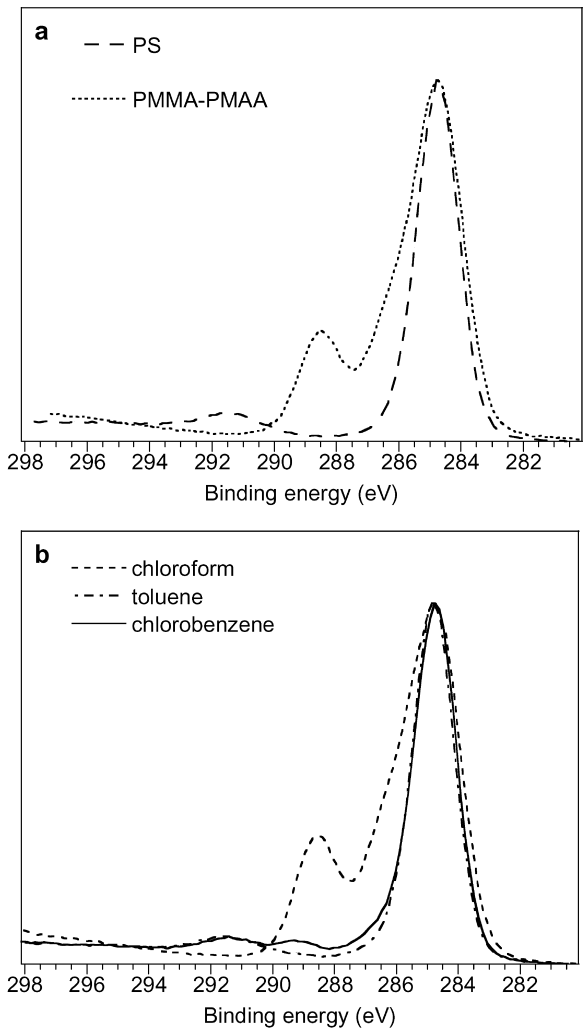

Fig. 3. C_{1s} spectra of PS and PMMA–PMAA (a) and spectra obtained after spin-coating PMMA–PMAA on PS from solutions (10 g/l) in chloroform, toluene and chlorobenzene (b). The spectra were normalized to bring the main component to the same height.

this moment. All this process takes place very quickly, leading to a relatively disordered surface morphology.

The surface tensions of PS and PMMA are not very different and the sign of the difference varies according to the method used for the evaluation [15,16]. Therefore, one cannot foresee what polymer should be exposed to the interface at equilibrium; moreover the surface composition of a spin-coated film may be different from that at equilibrium.

The main features observed with the high molecular mass PMMA and the low molecular mass PMMA–PMAA are similar. Here, the differences in molecular mass do not seem to be of major importance. The acidic functions may influence the behavior of PMMA–PMAA, but this is probably limited because these functions constitute a very small part of the polymer.

Chloroform has a high vapor pressure (18.6 kPa at room temperature [17]) and is the most volatile among the solvents used. The high concentration of the acrylic polymer at the surface may be due to the fact that PS has not enough time to dissolve. However the difference of relief between PMMA and PMMA–PMAA containing systems indicates that more subtle factors are involved as discussed in the literature [4,7].

Toluene and chlorobenzene have a vapor pressure of respectively 2.8 and 1.2 kPa at room temperature [17], and thus a markedly lower volatility compared to chloroform. PS is dissolved, and the surface in constituted of PS with inclusions of the acrylic polymer. Most probably, the separation is not absolute, a small fraction of one polymer being present in the other polymer phase, as commonly seen in phase diagrams.

Table 2 lists the Hildebrand solubility parameters of the solvents and the polymers used [18]. Data were not available for the PMMA–PMAA copolymer. The solubility of a polymer increases when its solubility parameter is closer to that of the solvent. PS is more soluble in toluene than PMMA; this explains that the surface obtained is almost entirely constituted of PS. In contrast, PMMA is more soluble than PS in chlorobenzene. A smaller amount of PS is dissolved and both polymers are found at the surface, by a process sketched in Fig. 7. In the first step, the polyacrylic polymer solution drop spreads on the substratum and the solvent begins to dissolve the PS. In the second step, demixing between PS and polyacrylic polymer occurs; the two polymers are swelled with the solvent. Finally, the solvent evaporates totally, and densification leads to edge formation between PS and the polyacrylic inclusions at the surface (step 3).

The evolution of the liquid phase composition during the spin-coating depends on numerous processes (PS dissolution, solvent evaporation, polymer demixing), which explains the variability observed in the size and concentration of the inclusions.

5. Conclusion

In this study, a common technique, the spin-coating, was used in a non conventional manner: a solution containing only one polymer (PMMA) was used, the other polymer

Table 2
Hildebrand solubility parameters δ of the different polymers and solvents used

	δ
PS	9.1
PMMA	9.5
Toluene	8.9
Chloroform	9.3
Chlorobenzene	9.5

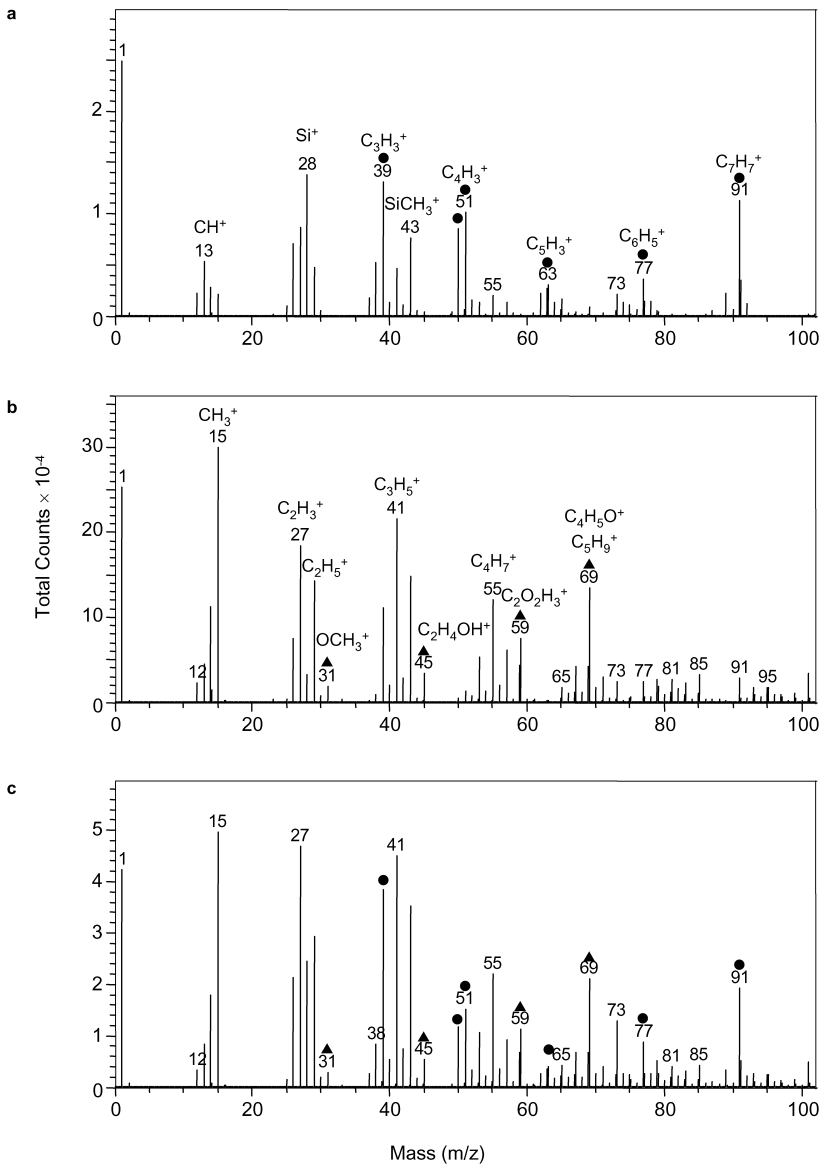

Fig. 4. Positive ToF-SIMS spectra of pure PS (a) and pure PMMA–PMAA (b), and spectrum obtained after spin-coating PMMA–PMAA on PS from a solution (10 g/l) in chlorobenzene (c): ●, peaks characteristic of PS; ▲, peaks characteristic of PMMA.

(PS) was dissolved from the surface. This method allowed heterogeneous surfaces to be created, with a very slight relief, depending on the solvent used. With chloroform, the surface was mainly covered with PMMA, while toluene gave a surface where PMMA was in low concentration. The use of chlorobenzene provided PMMA inclusions in a PS surface. The same observations were made with the PMMA–PMAA copolymer. The diameter of the PMMA–PMAA inclusions obtained with chlorobenzene was comprised between 150 nm and 1.5 μm. Their thickness was in the range above 100 nm. The acidic functions of the copolymer could be used for the grafting of various molecules of interest, for instance in the field of biocompatibilisation [19,20,21].

Acknowledgements

We thank the late P. Grange and P. Bertrand for the use of the atomic force microscopy and of the spin-coater, respectively, C. Poleunis and P. Bertrand for the ToF-SIMS analyses, A. Kaivez for the Gel Permeation Chromatography analyses and J. Devaux for fruitful discussions. Ch. Dupont-Gillain is a postdoctoral researcher of the Belgian National Foundation for Scientific Research (FNRS). The support of the FNRS, of the Federal Office for Scientific, Technical and Cultural Affairs (Interuniversity Poles of Attraction Program) and of the Research Department of the Communauté Française de Belgique (Concerted Research Action) is gratefully acknowledged.

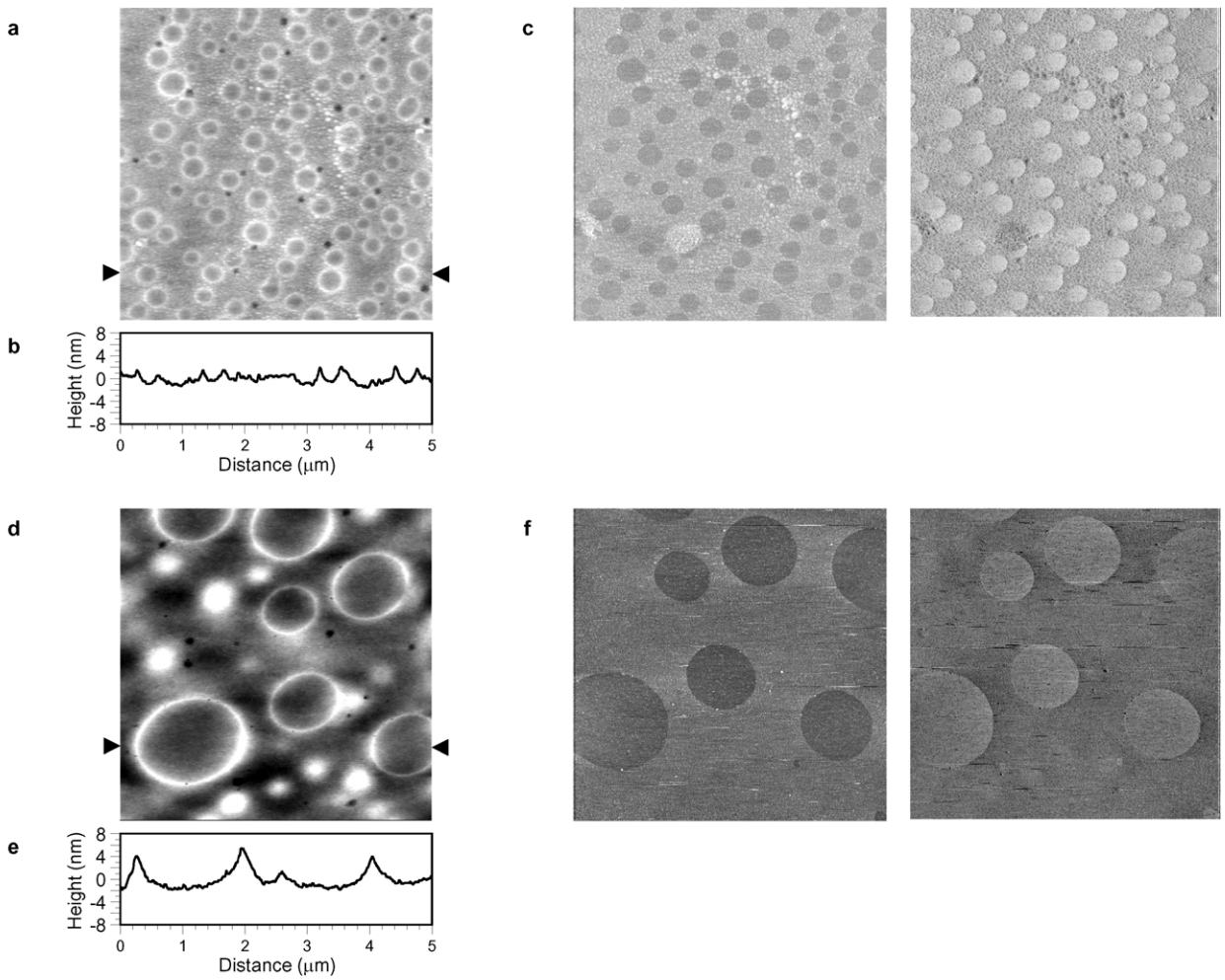

Fig. 5. AFM images ($5 \times 5\ \mu m^2$) obtained after spin-coating PMMA–PMAA on PS from a solution (10 g/l) in chlorobenzene, showing two extreme situations obtained on different samples. (a) and (d) Height (z-range = 10 nm); (b) and (e), section (indicated by the arrows in the height images); (c) and (f) friction (trace and retrace, z-range = 0.07 V).

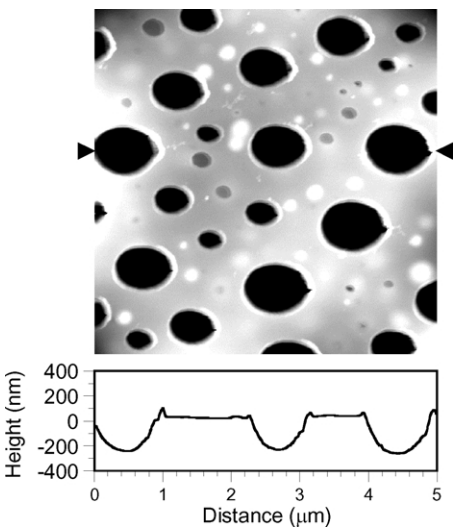

Fig. 6. AFM height image ($5 \times 5\ \mu m^2$) obtained after spin-coating PMMA–PMAA on PS from a solution (10 g/l) in chlorobenzene and selective dissolution of the PMMA–PMAA (z-range = 100 nm; section indicated by the arrows in the height image).

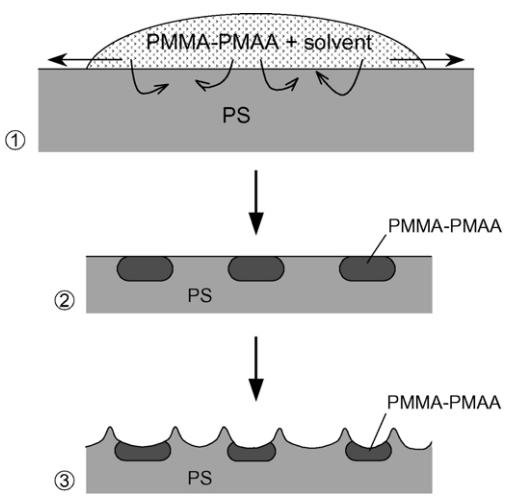

Fig. 7. Model describing the phase separation during the spin-coating process.

References

[1] Paul DR, Newman S, editors. Polymer blends, Vols. I and II. New York: Academic Press; 1978.

[2] Folkes MJ, Hope PS, editors. Polymer blends and alloys. Glasgow; Chapman and Hall: 1993.

[3] Wilkinson CDW, Riehle M, Wood M, Gallagher J, Curtis ASG. Mater Sci Engng C 2002;19:263–9.

[4] Ton-That C, Shard AG, Teare DOH, Bradley RH. Polymer 2001;42: 1121–9.

[5] Ton-That C, Shard AG, Daley R, Bradley RH. Macromolecules 2000; 33:8453–9.

[6] Tanaka K, Takahara A, Kajiyama T. Macromolecules 1996;29: 3232–9.

[7] Walheim S, Böltau M, Mlynek J, Krausch G, Steiner U. Macromolecules 1997;30:4995–5003.

[8] Takahara A, Nakamura K, Tanaka K, Kajiyama T. Macromol Symp 2000;159:89–96.

[9] Tanaka K, Takahara A, Kajiyama T. Macromolecules 1998;31: 863–9.

[10] Dewez JL, Doren A, Schneider YJ, Rouxhet PG. Biomaterials 1999; 20:547–59.

[11] Alaerts JA, De Cupere VM, Moser S, Van den Bosch de Aguilar P, Rouxhet PG. Biomaterials 2001;22:1635–42.

[12] Vickerman JC, Briggs D, Henderson A. The static SIMS library. Manchester: SurfaceSpectra Ltd; 1999. Part 2—Organic materials.

[13] Meine K, Schneider T, Spaltmann D, Santner E. Wear 2002;253: 725–32.

[14] Meine K, Schneider T, Spaltmann D, Santner E. Wear 2002;253: 733–8.

[15] Motomatsu M, Nie HY, Mizutani W, Tokumoto H. Jpn J Appl Phys 1994;33:3775–8.

[16] Wu S. Polymer interface and adhesion. New York: Marcel Dekker; 1982. Chapter 5.

[17] Weast RD. Handbook of chemistry and physics. Cleveland: The chemical Rubber Co; 1971. p. C-75–C-542.

[18] Grulke EA. Solubility parameters values. In: Brandrup J, Immergut EH, editors. Polymer handbook, 3rd ed. New York: Wiley; 1989. p. VII-519–VII-559.

[19] Noiset O, Schneider YJ, Marchand-Brynaert J. J Polym Sci: Part A: Polym Chem 1997;35:3779–90.

[20] Noiset O, Schneider YJ, Marchand-Brynaert J. J Biomater Sci Polym Ed 2000;11:767–86.

[21] Marchand-Brynaert J, Detrait E, Noiset O, Boxus T, Schneider YJ, Remacle C. Biomaterials 1999;20:1773–82.